Published in final edited form as:
Hippocampus. 2010 January ; 20(1): 113–124. doi:10.1002/hipo.20589.

Structural Plasticity of Dentate Granule Cell Mossy Fibers During the Development of Limbic Epilepsy

Steve C. Danzer[1,2,*], **Xiaoping He**[3], **Andreas W. Loepke**[1,2], and **James O. McNamara**[3,4,5,*]

[1] Department of Anesthesia, Cincinnati Children's Hospital Medical Center, Cincinnati, Ohio

[2] Departments of Anesthesia and Pediatrics, University of Cincinnati, Cincinnati, Ohio

[3] Department of Neurobiology, Duke University Medical Center, Durham, North Carolina

[4] Department of Medicine, Duke University Medical Center, Durham, North Carolina

[5] Department of Pharmacology and Cancer Biology, Duke University Medical Center, Durham, North Carolina

Abstract

Altered granule cell≫CA3 pyramidal cell synaptic connectivity may contribute to the development of limbic epilepsy. To explore this possibility, granule cell giant mossy fiber bouton plasticity was examined in the kindling and pilocarpine models of epilepsy using green fluorescent protein-expressing transgenic mice. These studies revealed significant increases in the frequency of giant boutons with satellite boutons 2 days and 1 month after pilocarpine status epilepticus, and increases in giant bouton area at 1 month. Similar increases in giant bouton area were observed shortly after kindling. Finally, both models exhibited plasticity of mossy fiber giant bouton filopodia, which contact GABAergic interneurons mediating feedforward inhibition of CA3 pyramids. In the kindling model, however, all changes were fleeting, having resolved by 1 month after the last evoked seizure. Together, these findings demonstrate striking structural plasticity of granule cell mossy fiber synaptic terminal structure in two distinct models of adult limbic epileptogenesis. We suggest that these plasticities modify local connectivities between individual mossy fiber terminals and their targets, inhibitory interneurons, and CA3 pyramidal cells potentially altering the balance of excitation and inhibition during the development of epilepsy.

Keywords

CA3; giant bouton; pilocarpine; kindling; dentate gate

INTRODUCTION

The entorhinal≫dentate≫hippocampal trisynaptic pathway is thought to play a central role in limbic epilepsy. Efforts to understand this role have produced the "dentate gate" hypothesis, which states that the granule cells of a normal brain block throughput of excess excitation from entorhinal cortex (EC) to downstream CA3 pyramids (Hsu, 2007). The discovery of limbic epilepsy-associated neuroplasticity of granule cells has fueled interest in this hypothesis. In particular, sprouting of granule cell mossy fiber axons into the dentate molecular layer (Nadler,

*Correspondence to: Steve C. Danzer, 3333 Burnet Avenue, ML 2001, Cincinnati, OH 45229-3039, USA. E-mail: steve.danzer@cchmc.org or James O. McNamara, 401 Bryan Research Building, Durham, NC 27705, USA. E-mail: jmc@neuro.duke.edu.

Additional Supporting Information may be found in the online version of this article.

2003), together with the accumulation of granule cells with basal dendrites (Spigelman et al., 1998; Ribak et al., 2000; Ribak and Dashtipour, 2002) contribute to the formation of aberrant recurrent excitatory connectivity among granule cells, essentially creating de novo dentate≫dentate circuits. These recurrent circuits are thought to disrupt the dentate gate.

In contrast to the extensive study of these examples of neuroplasticity within the dentate gyrus (DG) and hilus, however, plasticity within the primary mossy fiber projection into stratum lucidum of CA3, wherein mossy fibers innervate the apical dendrites of CA3 pyramids, has received less attention. Intriguingly, kindling and neonatal seizure-induced sprouting of mossy fiber axons into CA3 stratum oriens has been described (Represa and Ben-Ari, 1992; Holmes et al., 1999). Although it is likely that this sprouting originates from fibers in stratum lucidum, the extent to which these parent fibers also exhibit plastic changes is not known. Naturally, output of excessive excitation to the next component of the trisynaptic circuit is a critical aspect of the dentate gate hypothesis. Indeed, modeling studies suggest that for recurrent circuitry within the DG to disrupt the dentate gate, it must occur in combination with an enhancement of dentate output (Morgan and Soltesz, 2008). This finding suggests that pro-epileptogenic structural changes may manifest as alterations in dentate≫CA3 connectivity, underscoring the importance of determining whether the mossy fiber axons within stratum lucidum undergo structural neuroplasticity in limbic epileptogenesis.

Dentate granule cells directly excite CA3 pyramidal cells via their giant mossy fiber boutons, and indirectly inhibit CA3 pyramids by activating GABAergic inter-neurons through filopodial extensions arising from the giant boutons (Lawrence and McBain, 2003). In the adult mammalian brain, this connectivity is remarkably plastic (Galimberti et al., 2006). Local terminal arborization complexes formed by mossy fiber giant boutons with CA3 pyramids undergo striking increases in size and complexity as a function of environmental enrichment in the adult. Parallel studies in vitro reveal that these increases are dependent on neuronal activity and release of transmitters from mossy fiber terminals. Notably, enhanced firing of dentate granule cells occurs during limbic epileptogenesis (Labiner et al., 1993; Peng and Houser, 2005; Bower and Buckmaster, 2008). We therefore hypothesized that limbic epileptogenesis would be associated with increased size and complexity of giant mossy fiber boutons. To test this hypothesis, we used Thy1-GFP expressing transgenic mice to examine the structure of granule cell mossy fiber terminals in two animal models of limbic epileptogenesis, kindling, and pilocarpine-status epilepticus.

MATERIALS AND METHODS

All procedures conformed to NIH and institutional guidelines for the care and use of animals.

Thy1-GFP Expressing Mice

Mice expressing green fluorescent protein (GFP) under control of the Thy1 promoter were obtained as a generous gift from Dr. Guoping Feng (Duke University). The mice used in the present study were bred from the M line on a C57BL/6 background, and have been described previously (Feng et al., 2000; Danzer and McNamara, 2004; Walter et al., 2007; Danzer et al., 2008). Importantly, the subset of granule cells (~11%) that express GFP in this mouse line is morphologically and physiologically indistinguishable from unlabeled granule cells (Vuksic et al., 2008), and therefore is likely representative of the entire population.

Pilocarpine Model

Two to three-month-old GFP-expressing male and female mice were injected with 1 mg/kg methyl scopolamine nitrate intraperitoneally (i.p.). Fifteen minutes later, mice were injected i.p. with either 340 mg/kg pilocarpine or saline (control mice). All treatments occurred between

10 a.m. and noon. Mice were observed following the injections for the onset of status epilepticus, which typically occurred within 1 h. Status epilepticus was defined behaviorally by continuous tonic/clonic convulsions. Mice received 10 mg/kg diazepam 3 h after the onset of status epilepticus. Control mice received diazepam 4 h after saline injections. Pilocarpine-treated animals that failed to develop or did not survive status epilepticus were excluded from the study. Following status epilepticus, and for the next 2 days (once per day), animals were weighed and given Ringers solution as needed to maintain pre-seizure body weight. Each pilocarpine-treated animal was paired to a control animal, and the control animal received 0.5 ml Ringers if the pilocarpine-treated animal received an injection. Mice were perfused with paraformaldehyde 2 days (control, $N = 4$; status epilepticus, $N = 6$) or 1 month (control, $N = 7$; status epilepticus, $N = 12$) after treatment.

Kindling Model

Two to three-month-old GFP-expressing mice underwent stereotaxic implantation of a bipolar stimulation-recording electrode in the right amygdala under pentobarbital anesthesia (60 mg/kg, i.p.). The following coordinates were used, with bregma as reference: 1.0 mm posterior, 2.9 mm lateral, and 4.6 mm below dura. A wire secured to the skull overlying the left frontal cortex was used as a ground electrode. Electrographic seizure threshold was determined 1 week after surgery by application of a 1 s train of 1 ms biphasic rectangular pulses at 60 Hz beginning at 60 μA. Additional stimulations increasing by 20 μA were delivered at 1 min intervals until an electrographic seizure lasting at least 5 s was detected. Subsequently, experimental animals were stimulated twice a day at stimulus intensities 100 μA above the electrographic seizure threshold. Interstimulus interval was at least 4 h, and animals were stimulated each day until five consecutive seizures involving at least 12 s of limb clonus and/or tonus were evoked. Sham kindled animals were connected twice daily to the stimulation apparatus, but did not receive stimulations. Mice were perfused with paraformaldehyde 1 day (control, $N = 7$; kindled, $N = 7$) or 1 month (control, $N = 8$; kindled, $N = 7$) after the last kindled seizure or sham stimulation.

Perfusions

Animals were overdosed with 100 mg/kg pentobarbital administered i.p. and perfused through the ascending aorta at 10 ml/min for 30 s with ice-cold phosphate-buffered saline [phosphate buffered saline (PBS)] with 1 mM sodium orthovanadate (NaOV) and 1 U/ml heparin. Mice were then perfused for 10 min with 25°C, 2.5% paraformaldehyde, 4% sucrose, and 1 mM NaOV, pH 7.4. The brains were removed and post-fixed in the same fixative for 1 h at 4°C. Brains were cryoprotected in an ascending sucrose series (10%, 20%, 30%) in 1 mM NaOV in PBS, snap-frozen in isopentane cooled to −25°C with dry ice and stored at −80°C until cryosectioning. Forty micron coronal sections corresponding roughly to figure 46–48 of Paxinos and Franklin's mouse brain atlas (2001) were used for GFP, Nissl, and Fluoro-Jade B staining.

Microscopy and Data Collection

The following general guidelines were used for all image collection and data analysis. All images and analysis were collected with the investigator blinded to treatment group. Only bright GFP-labeled granule cells, in which processes could be followed to their natural terminations, were selected for analysis. GFP-expressing dentate granule cells were imaged using a Leica TCS SL confocal system set up on a Leica DMIRE2 inverted microscope equipped with epifluorescent illumination and a 63X oil immersion objective (NA 1.4). Using this system, three-dimensional Z-series stacks were captured at 0.2 μm increments with two to six times optical zoom. No corrections were made for shrinkage of the tissue. To avoid pseudoreplication, multiple measurements from individual animals were averaged and used as a single data point for statistical analysis. Significance was determined by Student's *t*-test.

Nonparametric versions of tests and medians and ranges are reported, as noted, for data that was not normally distributed. Finally, all comparisons were made between an experimental group and an age and condition-matched littermate control group. Control groups for the kindling and pilocarpine models differ by a number of variables (surgery, handling, etc.), so comparisons between controls should be avoided.

Mossy Fiber Axons

Confocal microscopy was used to image mossy fiber axons of dentate granule cells in stratum lucidum of CA3b (as defined by Lorente de Nó, 1934). Mossy fiber axons are decorated with three morphologically distinct types of presynaptic terminals; giant mossy fiber boutons, filopodial extensions arising from these giant boutons, and *en passant* terminals. Mossy fiber terminal structure was quantified by importing confocal image stacks into Neurolucida (Microbrightfield, Williston, VT) or Metamorph (Universal Imaging Corporation, West Chester, PA, version 4.5r6) imaging software. For this analysis, giant mossy fiber boutons were defined as expansions of the mossy fiber axon with a cross-sectional area that exceeded 4 μm^2 (Claiborne et al., 1986; Acsády et al., 1998). Electron microscopy studies indicate that these larger expansions are giant mossy fiber boutons, whereas expansions with a cross-sectional area of less than 4 μm^2 are *en passant* terminals, accumulations of mitochondria, or tissue artifacts (Acsády et al., 1998). Given the ambiguity about the identity of these smaller structures, only the larger giant mossy fiber boutons were examined here. Filopodia were defined as extensions arising from a giant mossy fiber bouton, but distinct from the main mossy fiber axon, that were less than 1 μm in diameter and greater than 1 μm in length (Amaral, 1979; Amaral and Dent, 1981). Filopodia were not included as part of the giant mossy fiber boutons cross sectional area. Recent data also demonstrate that giant mossy fiber boutons can be arranged into local terminal arborization complexes, consisting of a core mossy fiber giant bouton connected to one or more satellite boutons by axonal fibers originating from the core bouton (Galimberti et al., 2006). For the present study, satellites were defined as mossy fiber expansions connected to a core giant bouton by thin axonal processes. A profile area greater than 4 μm^2 was required for an expansion to qualify as a satellite, thereby distinguishing satellites from filopodia. Furthermore, only giant boutons in which all the emanating processes could be identified as either the primary axon, or followed to a natural termination as either a filopodium or satellite, were scored for determining the frequency of complexes. Because larger complexes, with more distant satellites, are more likely to be truncated in brain tissue sections, this conservative approach likely underestimates the frequency of complexes with satellites. Conservative criteria are necessary, however, since giant boutons are frequently penetrated by other axons (Rollenhagen et al., 2007), which could lead to overestimates of complex frequency.

Approximately 15–30 randomly-selected giant mossy fiber boutons from each animal were examined to determine mean cross sectional area, the percentage of giant mossy fiber boutons with satellites, filopodia number, and length. Two to four adjacent brain sections from each animal were used. To be selected for analysis, giant mossy fiber boutons had to be contained within the tissue section examined. The density of giant mossy fiber boutons per length of axon was determined from five to six axonal segments per animal, with a combined length of ~500–1,000 μm.

GFP Positive Cell Counts

The number and location of GFP-expressing granule cells in kindled and control mice was determined using Neurolucida software to analyze confocal image stacks. Images were collected with a Leica SP5 confocal microscope set up on a DMI6000 stand equipped with 10X objective (NA 0.3). Images were collected at 2 μm increments through the Z-depth of the DG. Neurolucida software was used to generate 3-dimensional reconstructions encoding the

number of GFP-expressing granule cells in the upper blade of the dentate in each section, the distance of each cell from the granule cell layer-hilar border and the distance of each cell from the crest of the DG. Importantly, measurements of GFP cell number and position were conducted in the same sections used for morphological studies. Finally, measurements presented here should not be construed as being representative of regions of the dentate not examined.

Cell Loss Scoring

Sections adjacent to those used for morphological studies were stained for Nissl substance with cresyl violet and cell loss was scored under 10× magnification in four regions: the hilus, dentate granule cell layer, CA3 pyramidal cell layer, and CA1 pyramidal cell layer. Regions were scored using a semiquantitative system as follows: 0: no obvious cell loss. 1: less than 25% cell loss. 2: ~50% cell loss. 3: greater than 90% cell loss. Two adjacent hippocampal sections per animal were scored, the scores for each region averaged and a cumulative cell loss score given to the animal (cumulative cell loss = hilus + dentate + CA3 + CA1; minimum possible score = 0, maximum = 12).

Fluoro-Jade B Staining

Fluoro-Jade B is a sensitive marker for dead and dying neurons (Schmued and Hopkins, 2000). To stain sections with Fluoro-Jade B, slides were immersed in 100% EtOH for 3 min, 70% EtOH for 1 min, dH2O for 1 min, 0.06% potassium permanganate for 15 min, dH2O for 1 min, 0.001% Fluoro-Jade B + 0.1% acetic acid for 30 min, rinsed in dH2O, air dried, and coverslipped with Crystalon. For each time point and epilepsy model, sections from control and experimental animals were stained simultaneously in the same containers. Sections from animals previously demonstrated to exhibit extensive cell loss, and sections from untreated animals were included with each reaction as positive and negative controls, respectively.

Figure Preparation

Confocal image stacks representing the z-depth of a neuronal structure were captured using a Leica TCS SL confocal microscope. Image stacks were used to generate maximum projections in Leica's LCS Lite Confocal software (version 2.61). In some cases, images are montages generated from the confocal z-series of a structure. This processing was done to remove adjacent structures located above or below the observed structure, which would obscure the two-dimensional representation. Montages, contrast, and brightness adjustments and figure preparation were conducted using Adobe Photoshop (version 7.0). Contrast and brightness were adjusted identically for images meant for comparison.

RESULTS

Part I: Dentate Granule Cell Structural Changes Following Pilocarpine-Induced Status Epilepticus

Increased giant mossy fiber bouton area and complexity following status epilepticus—Each dentate granule cell contacts ~15–20 CA3 pyramidal cells via giant mossy fiber boutons spaced along their mossy fiber axons (Amaral et al., 2007). At each contact point, either a single giant mossy fiber bouton or a complex of giant boutons is present. Changes in granule cell≫CA3 pyramidal cell connectivity may be reflected by altered density of giant mossy fiber boutons, by altered giant bouton area, or by the conversion of individual giant boutons into mossy fiber boutons with satellites. Strikingly, in the present study two of these three measures were significantly increased following status epilepticus. Two days after status, the percentage of giant boutons connected to satellite boutons was increased almost 3-fold over control values (Fig. 1, Table 1; $P = 0.049$); and 1 month after status, a more than 5-fold increase

was observed (Fig. 1, Table 1; $P = 0.009$). Moreover, giant mossy fiber bouton cross-sectional area was increased 37% relative to controls 1 month after status (Fig. 2; Table 1; $P = 0.010$). In contrast, the density of giant boutons along the mossy fiber axon was not altered at either time following status epilepticus (Table 1; single giant mossy fiber boutons and complexes were counted as one for this analysis).

Increased giant mossy fiber bouton filopodia number and length following status epilepticus—Filopodia exhibited substantial plasticity following status epilepticus. The number of filopodia emerging from a given giant mossy fiber bouton was increased 115% ($P = 0.049$) 2 days after status epilepticus, and 121% ($P = 0.006$) 1 month after status (Fig. 2; Table 1). Filopodia also tended to be longer following status epilepticus relative to control animals, and this effect was significant at 1 month (Fig. 2; Table 1; $P = 0.002$). Interestingly, changes in filopodia exhibited considerable heterogeneity throughout the population of giant mossy fiber boutons; reported averages (values for 15–30 giant boutons/animal were averaged for statistical analysis) tend to underestimate the dramatic changes among a subset of boutons. In control animals, for example, the longest filopodium observed was 5.64 and 5.50 μm at 2 days and 1 month, respectively. In contrast, after status, the longest filopodium observed was 24.1 and 31.9 μm at 2 days and 1 month, respectively. This effect is depicted graphically in Figure 3, which shows the length for each individual filopodium in each group.

Variable patterns of cell loss 1 month after status epilepticus—Because cell loss may contribute to changes in granule cell morphology, cell loss was assessed by both Fluoro-Jade B and Nissl stains. Two days after pilocarpine-status epilepticus, mice exhibited a consistent pattern in which extensive loss was evident in the hilus, and scattered cell loss was evident in the cortex and the CA1 and CA3 pyramidal cell layers (Fig. 4). This pattern of cell loss was similar to that observed in previous studies (Shibley and Smith, 2002;Borges et al., 2003). In contrast to the consistent pattern among animals at 2 days, striking variability in loss of principal cells was evident among animals sacrificed 1 month after status epilepticus. Four of the twelve pilocarpine-treated animals exhibited detectable cell loss only in the hilus 1 month after status, as evidenced by damage scores of 2 (see Fig. 5, middle column, for GFP, Fluoro-Jade B and Nissl staining from a representative animal). The remaining eight animals exhibited 25% or greater loss of cells in at least one principal cell layer in addition to loss of hilar cells (Fig. 5, right column). Cumulative damage scores for these animals ranged from 2.5 to 11. Five of the eight animals with principal cell loss exhibited increased Fluoro-Jade B labeling of hippocampal molecular layers [CA1 and CA3 stratum radiatum (SR) and oriens (SO)], (Fig. 5, right column, FJB row). Increased Fluoro-Jade B labeling was not evident in control animals or pilocarpine-treated animals exhibiting intact principal cell layers 1 month after status epilepticus (Fig. 5, left and middle columns, FJB row). Together, these findings suggest that neuronal degeneration continues in some animals in the days and weeks following status epilepticus, consistent with previous studies (Peredery et al., 2000;Poirier et al., 2000;Nairismägi et al., 2004).

Cell loss is correlated with changes in granule cell morphology—The striking heterogeneity in the extent of principal cell loss among animals studied 1 month after status epilepticus led us to query whether there may be a correlation between the structural modifications of the granule cells and the extent of cell death. These analyses revealed that cell loss was indeed correlated with some, but not all, changes in granule cell synaptic terminal structure. That is, cumulative damage scores for each animal were significantly correlated with the percentage of giant mossy fiber boutons connected to satellite boutons (MFB complexes) and with giant mossy fiber bouton area. Correlation coefficients (R) and respective P-values for each variable are presented in supplemental Table 1 (top row). By contrast, cumulative damage scores were not significantly correlated with giant mossy fiber bouton density,

filopodia number, or filopodia length. Importantly, only pilocarpine-treated animals were included in these analyses, so positive correlations reflect differences in the amount of cell death following status epilepticus rather than differences between control animals (with no cell death) and pilocarpine-treated groups.

The relationship between cell loss and granule cell morphology was complex. The percentage of giant boutons with satellites increased with greater cell loss, whereas giant mossy fiber bouton area decreased with greater cell loss (Fig. 6). With respect to giant mossy fiber bouton area in particular, inclusion of control animals in the analysis (controls denoted by asterisks in Fig. 6) revealed a bimodal relationship, in that the largest giant boutons were present in pilocarpine-treated animals with minimal cell loss when compared with control animals or pilocarpine-treated animals with more extensive cell loss. A post hoc analysis comparing pilocarpine-treated animals with no obvious loss of principal cells ($N = 4$) to control animals ($N = 7$) and to pilocarpine-treated animals with obvious loss of principal cells ($N = 8$) revealed that giant mossy fiber bouton profile area was significantly increased relative to these latter groups (SE, minimal cell loss, 12.8 ± 0.7 μm^2; control, 7.9 ± 0.4; SE, extensive cell loss, 9.9 ± 0.9; analysis of variance (ANOVA) with Tukey post test, $P = 0.002$ vs. control, $P = 0.04$ vs. SE with extensive loss). Mossy fiber axons and giant boutons (denoted by asterisks) from animals with either no overt or obvious loss of principal cells are shown in Figure 7 (top and bottom, respectively). The smaller giant boutons evident in the animal with obvious cell loss are associated with “beaded” axons; an appearance likely reflecting degenerative changes following target cell loss (Nadler et al., 1981).

Finally, although it seems likely that loss of particular principal cell layers would be associated with specific changes in granule cell morphology, it was not possible to draw any clear conclusions from the present data. This was because cell loss in any one layer was highly correlated with cell loss in almost all other layers (see supplemental Table 2). Dissociating the impact of loss of CA3 pyramidal cells from loss of CA1 pyramidal cells, for example, was thus not possible in these animals. Nevertheless, positive correlations between loss of specific cell layers and changes in granule cell morphology are presented in supplemental Table 1. Given the above caveats, however, these findings should be interpreted with caution.

Part 2: Dentate Granule Cell Structural Changes Following Kindling-Epileptogenesis

Mice in the kindling protocol received two stimulations per day until five consecutive seizures of class four or five were evoked, requiring an average of 22 ± 3.4 stimulations for animals sacrificed 1 day after the last evoked seizure, and 17 ± 2.2 stimulations for animals taken 1 month after the last evoked seizure (groups did not differ; $P = 0.242$, *t*-test). Cumulative mean afterdischarge duration was 527 ± 101 and 397 ± 69 s for 1 day and 1 month animals, respectively ($P = 0.308$, *t*-test). The kindling paradigm used in the present study produces a lifelong enhanced response to the stimulation and also hyperexcitability in the hippocampus evident 1 month after the last stimulation (King et al., 1985). Importantly, this paradigm does not lead to recurrent seizures or produce widespread neuronal loss as occurs in the pilocarpine model; qualitative examination of Nissl and Fluoro-Jade B stains revealed no evidence of neuronal loss either 1 day or 1 month after the last kindled seizure (not shown). Notably, small numbers of TUNEL-reactive neurons have been described in the dentate hilus of animals undergoing few kindled seizures (Bengzon et al., 1997; Pretel et al., 1997; Umeoka et al., 2000; Gawłowicz et al., 2006); however, no reductions of hilar neuron number were detected following kindled seizures evoked by stimulation of amygdala (Watanabe et al., 1996; Tuunanen and Pitkanen, 2000) although an increase of hilar volume was detected by Watanabe et al. (1996).

Increased giant mossy fiber bouton area following kindling—Reminiscent of animals following status epilepticus, 1 day after the last evoked seizure giant mossy fiber bouton area was increased by 48% relative to controls (Table 2, *P*Fig. 8; = 0.013). In contrast to pilocarpine-treated animals, this change was transient. One month after the last kindled seizure, giant mossy fiber bouton area did not differ from controls (Table 2). Neither the density of giant boutons per length of axon, nor the percentage of giant boutons connected to satellite boutons was significantly altered in kindled animals at either time point.

Increased giant mossy fiber bouton filopodia number and length following kindling—The number of filopodia possessed by a given giant mossy fiber bouton was increased by 61%, 1 day after the last kindled seizure (Fig. 8; Table 2; $P = 0.044$). Filopodia were also significantly longer 1 day after the last kindled seizure ($P = 0.014$). Again, however, these changes were transient, and 1 month after the last kindled seizure, filopodia number and length were indistinguishable from controls (Fig. 8; Table 2). Interestingly, although mean filopodia length was increased after kindling, the incidence of very long filopodia was low (Fig. 9) compared with pilocarpine-treated animals. Indeed, the longest filopodium from a kindled animal was only 15.75 μm, half the length of the longest filopodium (31.9 μm) from a poststatus animal.

The number and distribution of GFP-labeled granule cells was equivalent in control and kindled mice—In the present study, care was taken to confirm that similar populations of dentate granule cells were labeled with GFP in control and kindled mice. GFP expression in these animals is driven by the Thy1 promoter, a member of the Ig superfamily, and it is possible that kindling stimulations might alter the activity of the Thy1 promoter. To examine this possibility, the number and position of GFP-labeled dentate granule cells in control and kindled mice was determined. One day after the completion of kindling or sham kindling, 30.4 ± 9.1 (control, mean ± sem) and 31.1 ± 6.0 (kindled) granule cells were labeled with GFP in the superior blade of the dentate. These neurons were on average 37.7 ± 3.5 and 41.1 ± 2.5 μm from the granule cell layer/hilar border, and 598 ± 52 and 650 ± 40 μm, respectively, from the crest of the dentate. Granule cell number and location was also similar 1 month after the completion of kindling or sham kindling (control, 12.9 ± 5.6 granule cells/superior blade, 37.8 ± 2.1 μm from hilar border, 714 ± 56 μm from crest; kindled, 16.4 ± 6.9, 34.6 ± 3.6 μm, 714 ± 50 μm). These findings indicate that similar populations of granule cells were labeled with GFP in kindled mice and their respective control groups, and that morphological differences between groups reflect real changes in neuronal structure.

DISCUSSION

Here, we tested the hypothesis that limbic epileptogenesis would increase the size and complexity of granule cell giant mossy fiber boutons. Consistent with this hypothesis, the frequency of giant boutons with satellite boutons was increased 2 days and 1 month after status epilepticus, and giant bouton area was increased 1 month after status. Similarly, increases in giant bouton area were observed shortly after kindling. In the kindling model, however, all changes were fleeting, having resolved by 1 month after the last evoked seizure. Together, these findings demonstrate striking mossy fiber giant bouton plasticity in two distinct models of adult limbic epileptogenesis. We suggest that these changes modify local connectivities between individual giant boutons and CA3 pyramidal cells, thereby facilitating synaptic activation of CA3 pyramids in these models.

Giant mossy fiber bouton filopodia, which contact inhibitory interneurons in stratum lucidum, also exhibit plastic changes in both models of epilepsy. In the pilocarpine model, the number of filopodia per giant mossy fiber bouton was increased 2 days after status, and number and length were increased 1 month after status. Filopodia number and length were also increased

in the kindling model, but again, changes were only evident 1 day after the last seizure. Although the functional significance of filopodial neuroplasticity is less clear, it could reflect homeostatic mechanisms aimed at maintaining network stability.

To place these instances of mossy fiber synaptic neuroplasticity in a broader context, cell death was also examined in these animals. This led to the important finding that several components of mossy fiber terminal plasticity were highly correlated with the extent of hippocampal cell loss. This finding underscores the value of assessing cell loss in these models, and suggests that the dentate may play very different roles—even within an epilepsy model—depending on the integrity of surrounding tissues.

Neuronal Activity Regulates Mossy Fiber Terminal Plasticity

Recent time-lapse imaging studies of organotypic explant cultures have revealed that neuronal activity regulates the structure of mossy fiber terminals. Inclusion of either tetrodotoxin (which blocks action potentials) or DCG-IV (which blocks glutamate release from mossy fiber terminals) reduces the number of giant mossy fiber boutons with satellites in a reversible manner (Galimberti et al., 2006), whereas neuronal activity regulates filopodia dynamics in a glutamate-dependent fashion (De Paola et al., 2003; Tashiro et al., 2003). Because limbic seizures in both the kindling and status epilepticus models are accompanied by increased firing of granule cells (Labiner et al., 1993; Bragin et al., 1997; Peng and Houser, 2005; Bower and Buckmaster, 2008), it is likely that increased neuronal activity contributes to the instances of mossy fiber neuroplasticity described here. This proposal is consistent with the time courses observed. That is, increased neuronal activity occurs during the seizures evoked during development of kindling but remits thereafter because spontaneous seizures are not evident in this model; this correlates with the presence of structural changes 2 days but not 1 month after kindling. By contrast, increased neuronal activity would be expected to persist in the pilocarpine status epilepticus model because recurrent spontaneous seizures uniformly arise in C57BL/6 mice so treated (Shibley and Smith, 2002). Such increased activity may contribute to the persistent structural changes evident in these animals 1 month after status epilepticus. Importantly, the possibility that death of CA3 pyramids in the pilocarpine model also contributed to these instances of neuroplasticity seems plausible because of the excellent correlation between cell death and the appearance of satellites 1 month after status (Fig. 6). However, cell death is not required because simply exposing adult mice to an enriched environment increased the incidence of satellites (Galimberti et al., 2006).

Epileptogenesis Enhances Granule Cell≫CA3 Pyramidal Cell Connectivity

The dentate gate hypothesis holds that the development of limbic epilepsy is promoted by a failure of the dentate to limit throughput of excitatory activity from EC to the hippocampal pyramidal cells, thereby facilitating recruitment of the hippocampus into seizure activity (Hsu, 2007). Whether regulation of dentate granule cell≫CA3 pyramidal cell connectivity contributes to impaired gating is unclear. Giant mossy fiber boutons are the presynaptic structural component of the dentate granule cell≫CA3 pyramidal cell connection. Even under normal conditions, the giant mossy fiber bouton synapses with spines of CA3 pyramids are among the most potent synapses in the CNS, dubbed the “detonator” synapse for their ability to single-handedly fire target pyramidal cells (Henze et al., 2002). The present findings of increased giant bouton area and satellite frequency raise the possibility that this synapse is even more potent following epileptogenesis. Specifically, electron microscopy studies reveal that larger giant boutons contain larger active zones (Pierce and Milner, 2001), suggesting that these larger boutons will release more transmitter. Indeed, paired recordings of granule cells and CA3 pyramids in organotypic explant cultures reveal that activation of larger giant boutons produces larger amplitude EPSCs compared with smaller boutons (Galimberti et al., 2006). In addition to the potential of increased release of neurotransmitter at pre-existing synapses, the

formation of giant mossy fiber boutons with satellites in the pilocarpine model may increase the degree of divergence onto CA3 pyramidal cell dendrites and sharply focus information flow from individual spiking mossy fibers, selectively activating a subset of CA3 pyramids. The net result may be the emergence of microcircuits of preferentially interconnected dentate granule and CA3 pyramidal cells.

Electrophysiological studies of the mossy fiber≫CA3 pyramid synapse have begun to probe its functional status in hippocampal slices isolated after status epilepticus induced by kainic acid. Field potential recordings revealed decreased paired-pulse facilitation in slices isolated following status epilepticus compared with controls; the occlusion suggesting that this synapse had undergone long-term potentiation (LTP) in vivo (Goussakov et al., 2000). Notably, expression of LTP at this synapse is thought to be due to increased release of glutamate from mossy fiber terminals (Nicoll and Schmitz, 2005), implying a presynaptic locale for expression of this plasticity (but see also Kwon and Castillo, 2008; Rebola et al., 2008). The finding of enhanced glutamate release from synaptosomes prepared from the mossy fiber region of status epilepticus-treated animals further supports this assertion (Goussakov et al., 2000). Thus the efficacy of granule cell≫CA3 pyramidal cell synapses in this model appears to be enhanced and plasticity intrinsic to mossy fiber terminals is an important contributor to the enhancement. The increased giant bouton area and complexity described here may reflect structural underpinnings of these physiological changes. Our findings provide a strong rationale for correlative electrophysiological studies in the present models.

Epileptogenesis May Regulate Granule Cell≫stratum Lucidum Interneuron Connectivity

An important mechanism by which enhanced granule cell≫CA3 pyramidal cell connectivity could be blunted involves the filopodial extensions of the giant boutons. Filopodial extensions make contact with inhibitory interneurons (Amaral, 1979; Acsády et al., 1998), one role of which is to mediate feedforward inhibition of CA3 pyramidal cells (Frotscher, 1989; Vida and Frotscher, 2000; Mori et al., 2004). Indeed, the dentate is unusual in that inhibitory interneurons, rather than excitatory principal cells, are the major target of mossy fiber axons, in that mossy fibers innervate about 10 times as many interneurons as CA3 pyramidal cells (Acsády at al., 1998). The unusual strength of the granule cell≫pyramidal cell synapse may necessitate this ratio, and correspondingly, feedforward inhibition could play an important role in epileptogenesis. In the present study, increased numbers of filopodia were found in both the kindling and pilocarpine models; whether these form functional synapses with viable interneurons within stratum lucidum is uncertain. Indeed, the loss of inhibitory interneurons in the pilocarpine and lithium-pilocarpine models (Obenaus et al., 1993; Houser and Esclapez, 1996; Mello and Covolan, 1996; André et al., 2001; Covolan and Mello, 2006) raises the possibility that newly produced filopodia fail to form functional synapses. Perhaps the unusually long filopodia in the pilocarpine model simply reflect excess sprouting of afferent terminals seeking targets. Indeed, cell loss-induced changes in free extracellular space may promote increased filopodial motility (Tashiro et al., 2003). Electrophysiological studies of mossy fiber-mediated feedforward inhibition will be required to understand the functional significance of this structural plasticity.

Granule Cell Plasticity and the Development of Epilepsy

In the present study, granule cell plasticity was examined in the kindling and pilocarpine models of epilepsy, the former being characterized by hyperexcitability alone, and the latter by hyperexcitability and spontaneous seizures. In both models, giant boutons exhibited changes consistent with enhanced pyramidal cell excitation. In the kindling model, however, changes were fleeting, implying that structural plasticity of mossy fiber terminals does not underlie persistent hyperexcitability—evident as evoked seizures—in these animals. In contrast, changes were present both 2 days and 1 month after pilocarpine-status epilepticus, indicating

that these changes persist in the epileptic brain. Importantly, these structural changes occur within days, whereas spontaneous seizures take weeks to develop, does not exclude a pro-epileptogenic role of these changes. In principal, rapid pro-epileptogenic changes could be effectively offset in the short-term by compensatory changes aimed at maintaining homeostasis (Sainsbury et al., 1978). Dissipation of compensatory changes over time could allow seizure break-through. Indeed, previous studies suggest a morphological substrate for such a phenomenon. Shortly after status epilepticus, granule cells exhibit a dramatic loss of dendritic spines, a change predicted to inhibit seizures. Within weeks of the insult, however, spine density recovers (Isokawa, 1998; Isokawa, 2000), potentially exposing covert pro-epileptogenic changes. Finally, it is intriguing to note that previous studies using the pilocarpine model indicate that CA3 pyramidal cell loss is negatively correlated with the onset of chronic epilepsy (Mello et al., 1993); the implication being that preservation of this pathway, in combination with the changes described here, promotes epileptogenesis. Animals in which the CA3 pyramids are rapidly destroyed, and correspondingly, enhanced granule cell≫CA3 pyramidal cell connectivity is precluded, develop epilepsy by other, presumably less efficient, pathways.

Supplementary Material

Refer to Web version on PubMed Central for supplementary material.

Acknowledgments

NIH; Grant number: R01-NS-056217; Grant sponsors: Epilepsy Foundation, the Ruth K. Broad Foundation, and Cincinnati Children's Hospital Research Foundation.

The authors thank Keri Kaeding and Dr. Yangzhong Huang for their useful comments on the earlier versions of this manuscript.

References

Acsády L, Kamondi A, Sík A, Freund T, Buzsáki G. GABAergic cells are the major postsynaptic targets of mossy fibers in the rat hippocampus. J Neurosci 1998;18:3386–3403. [PubMed: 9547246]

Amaral DG. Synaptic extensions from the mossy fibers of the fascia dentata. Anat Embryol (Berl) 1979;155:241–251. [PubMed: 453543]

Amaral DG, Dent JA. Development of the mossy fibers of the dentate gyrus: I. A light and electron microscopic study of the mossy fibers and their expansions. J Comp Neurol 1981;195:51–86. [PubMed: 7204652]

Amaral DG, Scharfman HE, Lavenex P. The dentate gyrus: Fundamental neuroanatomical organization (dentate gyrus for dummies). Prog Brain Res 2007;163:3–22. [PubMed: 17765709]

André V, Marescaux C, Nehlig A, Fritschy JM. Alterations of hippocampal GAbaergic system contribute to development of spontaneous recurrent seizures in the rat lithium-pilocarpine model of temporal lobe epilepsy. Hippocampus 2001;11:452–468. [PubMed: 11530850]

Bengzon J, Kokaia Z, Elmér E, Nanobashvili A, Kokaia M, Lindvall O. Apoptosis and proliferation of dentate gyrus neurons after single and intermittent limbic seizures. Proc Natl Acad Sci USA 1997;94:10432–10437. [PubMed: 9294228]

Borges K, Gearing M, McDermott DL, Smith AB, Almonte AG, Wainer BH, Dingledine R. Neuronal and glial pathological changes during epileptogenesis in the mouse pilocarpine model. Exp Neurol 2003;182:21–34. [PubMed: 12821374]

Bower MR, Buckmaster PS. Changes in granule cell firing rates precede locally recorded spontaneous seizures by minutes in an animal model of temporal lobe epilepsy. J Neurophysiol 2008;99:2431–2442. [PubMed: 18322007]

Bragin A, Csicsvári J, Penttonen M, Buzsáki G. Epileptic after-discharge in the hippocampal-entorhinal system: Current source density and unit studies. Neuroscience 1997;76:1187–1203. [PubMed: 9027878]

Claiborne BJ, Amaral DG, Cowan WM. A light and electron microscopic analysis of the mossy fibers of the rat dentate gyrus. J Comp Neurol 1986;246:435–458. [PubMed: 3700723]

Covolan L, Mello LE. Assessment of the progressive nature of cell damage in the pilocarpine model of epilepsy. Braz J Med Biol Res 2006;39:915–924. [PubMed: 16862283]

Danzer SC, McNamara JO. Localization of brain-derived neurotrophic factor to distinct terminals of mossy fiber axons implies regulation of both excitation and feedforward inhibition of CA3 pyramidal cells. J Neurosci 2004;24:11346–11355. [PubMed: 15601941]

Danzer SC, Kotloski RJ, Walter C, Hughes M, McNamara JO. Altered morphology of hippocampal dentate granule cell presynaptic and postsynaptic terminals following conditional deletion of TrkB. Hippocampus 2008;18:668–678. [PubMed: 18398849]

De Paola V, Arber S, Caroni P. AMPA receptors regulate dynamic equilibrium of presynaptic terminals in mature hippocampal networks. Nat Neurosci 2003;6:491–500. [PubMed: 12692557]

Feng G, Mellor RH, Bernstein M, Keller-Peck C, Nguyen QT, Wallace M, Nerbonne JM, Lichtman JW, Sanes JR. Imaging neuronal subsets in transgenic mice expressing multiple spectral variants of GFP. Neuron 2000;28:41–51. [PubMed: 11086982]

Frotscher M. Mossy fiber synapses on glutamate decarboxylase-immunoreactive neurons: Evidence for feed-forward inhibition in the CA3 region of the hippocampus. Exp Brain Res 1989;75:441–445. [PubMed: 2721621]

Galimberti I, Gogolla N, Alberi S, Santos AF, Muller D, Caroni P. Long-term rearrangements of hippocampal mossy fiber terminal connectivity in the adult regulated by experience. Neuron 2006;50:749–763. [PubMed: 16731513]

Gawłowicz M, Reichert M, Wojcierowski J, Czuczwar SJ, Borowicz KK. Apoptotic markers in various stages of amygdala kindled seizures in rats. Pharmacol Rep 2006;58:512–518. [PubMed: 16963797]

Goussakov IV, Fink K, Elger CE, Beck H. Metaplasticity of mossy fiber synaptic transmission involves altered release probability. J Neurosci 2000;20:3434–3441. [PubMed: 10777806]

Henze DA, Wittner L, Buzsáki G. Single granule cells reliably discharge targets in the hippocampal CA3 network in vivo. Nat Neurosci 2002;5:790–795. [PubMed: 12118256]

Holmes GL, Sarkisian M, Ben-Ari Y, Chevassus-Au-Louis N. Mossy fiber sprouting after recurrent seizures during early development in rats. J Comp Neurol 1999;404:537–553. [PubMed: 9987996]

Houser CR, Esclapez M. Vulnerability and plasticity of the GABA system in the pilocarpine model of spontaneous recurrent seizures. Epilepsy Res 1996;26:207–218. [PubMed: 8985701]

Hsu D. The dentate gyrus as a filter or gate: A look back and a look ahead. Prog Brain Res 2007;163:601–613. [PubMed: 17765740]

Isokawa M. Remodeling dendritic spines in the rat pilocarpine model of temporal lobe epilepsy. Neurosci Lett 1998;258:73–76. [PubMed: 9875530]

Isokawa M. Remodeling dendritic spines of dentate granule cells in temporal lobe epilepsy patients and the rat pilocarpine model. Epilepsia 2000;41 (Suppl 6):S14–S17. [PubMed: 10999513]

King GL, Dingledine R, Giacchino JL, McNamara JO. Abnormal neuronal excitability in hippocampal slices from kindled rats. J Neurophysiol 1985;54:1295–1304. [PubMed: 3001236]

Kwon HB, Castillo PE. Long-term potentiation selectively expressed by NMDA receptors at hippocampal mossy fiber synapses. Neuron 2008;57:108–120. [PubMed: 18184568]

Labiner DM, Butler LS, Cao Z, Hosford DA, Shin C, McNamara JO. Induction of c-fos mRNA by kindled seizures: Complex relationship with neuronal burst firing. J Neurosci 1993;13:744–751. [PubMed: 8381172]

Lawrence JJ, McBain CJ. Interneuron diversity series: Containing the detonation–feedforward inhibition in the CA3 hippocampus. Trends Neurosci 2003;26:631–640. [PubMed: 14585604]

Lorente de Nó R. Studies on the structure of the cerebral cortex. II. Continuation of the study of the ammonic system. J Psychol Neurol (Lpz) 1934;46:113–177.

Mello LE, Cavalheiro EA, Tan AM, Kupfer WR, Pretorius JK, Babb TL, Finch DM. Circuit mechanisms of seizures in the pilocarpine model of chronic epilepsy: Cell loss and mossy fiber sprouting. Epilepsia 1993;34:985–995. [PubMed: 7694849]

Mello LE, Covolan L. Spontaneous seizures preferentially injure interneurons in the pilocarpine model of chronic spontaneous seizures. Epilepsy Res 1996;26:123–129. [PubMed: 8985694]

Morgan RJ, Soltesz I. Nonrandom connectivity of the epileptic dentate gyrus predicts a major role for neuronal hubs in seizures. Proc Natl Acad Sci USA 2008;105:6179–6184. [PubMed: 18375756]

Mori M, Abegg MH, Gähwiler BH, Gerber U. A frequency-dependent switch from inhibition to excitation in a hippocampal unitary circuit. Nature 2004;431:453–456. [PubMed: 15386013]

Nadler JV, Perry BW, Gentry C, Cotman CW. Fate of the hippocampal mossy fiber projection after destruction of its postsynaptic targets with intraventricular kainic acid. J Comp Neurol 1981;196:549–569. [PubMed: 7204671]

Nadler JV. The recurrent mossy fiber pathway of the epileptic brain. Neurochem Res 2003;28:1649–1658. [PubMed: 14584819]

Nairismägi J, Gröhn OH, Kettunen MI, Nissinen J, Kauppinen RA, Pitkänen A. Progression of brain damage after status epilepticus and its association with epileptogenesis: A quantitative MRI study in a rat model of temporal lobe epilepsy. Epilepsia 2004;45:1024–1034. [PubMed: 15329065]

Nicoll, Schmitz. Synaptic plasticity at hippocampal mossy fibre synapses. Nat Rev Neurosci 2005;6:863–876. [PubMed: 16261180]

Obenaus A, Esclapez M, Houser CR. Loss of glutamate decarboxylase mRNA-containing neurons in the rat dentate gyrus following pilocarpine-induced seizures. J Neurosci 1993;13:4470–4485. [PubMed: 8410199]

Paxinos, G.; Franklin, KB. The Mouse Brain in Stereotaxic Coordinates. London: Academic Press; 2001.

Peng Z, Houser CR. Temporal patterns of fos expression in the dentate gyrus after spontaneous seizures in a mouse model of temporal lobe epilepsy. J Neurosci 2005;25:7210–7220. [PubMed: 16079403]

Peredery O, Persinger MA, Parker G, Mastrosov L. Temporal changes in neuronal dropout following inductions of lithium/pilocarpine seizures in the rat. Brain Res 2000;881:9–17. [PubMed: 11033088]

Pierce JP, Milner TA. Parallel increases in the synaptic and surface areas of mossy fiber terminals following seizure induction. Synapse 2001;39:249–256. [PubMed: 11169773]

Poirier JL, Capek R, De Koninck Y. Differential progression of Dark Neuron and Fluoro-Jade labelling in the rat hippocampus following pilocarpine-induced status epilepticus. Neuroscience 2000;97:59–68. [PubMed: 10771339]

Pretel S, Applegate CD, Piekut D. Apoptotic and necrotic cell death following kindling induced seizures. Acta Histochem 1997;99:71–79. [PubMed: 9150799]

Rebola N, Lujan R, Cunha RA, Mulle C. Adenosine A2A receptors are essential for long-term potentiation of NMDA-EPSCs at hippocampal mossy fiber synapses. Neuron 2008;57:121–134. [PubMed: 18184569]

Represa A, Ben-Ari Y. Kindling is associated with the formation of novel mossy fibre synapses in the CA3 region. Exp Brain Res 1992;92:69–78. [PubMed: 1486956]

Ribak CE, Tran PH, Spigelman I, Okazaki MM, Nadler JV. Status epilepticus-induced hilar basal dendrites on rodent granule cells contribute to recurrent excitatory circuitry. J Comp Neurol 2000;428:240–253. [PubMed: 11064364]

Ribak CE, Dashtipour K. Neuroplasticity in the damaged dentate gyrus of the epileptic brain. Prog Brain Res 2002;136:319–328. [PubMed: 12143392]

Rollenhagen A, Sätzler K, Rodríguez EP, Jonas P, Frotscher M, Lübke JH. Structural determinants of transmission at large hippocampal mossy fiber synapses. J Neurosci 2007;27:10434–10444. [PubMed: 17898215]

Sainsbury RS, Bland BH, Buchan DH. Electrically induced seizure activity in the hippocampus: Time course for postseizure inhibition of subsequent kindled seizures. Behav Biol 1978;22:479–488. [PubMed: 697682]

Schmued LC, Hopkins KJ. Fluoro-Jade B: A high affinity fluorescent marker for the localization of neuronal degeneration. Brain Res 2000;874:123–130. [PubMed: 10960596]

Shibley H, Smith BN. Pilocarpine-induced status epilepticus results in mossy fiber sprouting and spontaneous seizures in C57BL/6 and CD-1 mice. Epilepsy Res 2002;49:109–120. [PubMed: 12049799]

Spigelman I, Yan XX, Obenaus A, Lee EY, Wasterlain CG, Ribak CE. Dentate granule cells form novel basal dendrites in a rat model of temporal lobe epilepsy. Neuroscience 1998;86:109–120. [PubMed: 9692747]

Tashiro A, Dunaevsky A, Blazeski R, Mason CA, Yuste R. Bidirectional regulation of hippocampal mossy fiber filopodial motility by kainate receptors: A two-step model of synaptogenesis. Neuron 2003;38:773–784. [PubMed: 12797961]

Tuunanen J, Pitkänen A. Do seizures cause neuronal damage in rat amygdala kindling? Epilepsy Res 2000;39:171–176. [PubMed: 10759304]

Umeoka S, Miyamoto O, Janjua NA, Nagao S, Itano T. Appearance and alteration of TUNEL positive cells through epileptogenesis in amygdaloid kindled rat. Epilepsy Res 2000;42 (2–3):97–103. [PubMed: 11074182]

Vida I, Frotscher M. A hippocampal interneuron associated with the mossy fiber system. Proc Natl Acad Sci USA 2000;97:1275–1280. [PubMed: 10655521]

Vuksic M, Del Turco D, Bas Orth C, Burbach GJ, Feng G, Müller CM, Schwarzacher SW, Deller T. 3D-reconstruction and functional properties of GFP-positive and GFP-negative granule cells in the fascia dentata of the Thy1-GFP mouse. Hippocampus 2008;18:364–375. [PubMed: 18189310]

Watanabe Y, Johnson RS, Butler LS, Binder DK, Spiegelman BM, Papaioannou VE, McNamara JO. Null mutation of c-fos impairs structural and functional plasticities in the kindling model of epilepsy. J Neurosci 1996;16:3827–3836. [PubMed: 8656277]

Walter C, Murphy BL, Pun RY, Spieles-Engemann AL, Danzer SC. Pilocarpine-induced seizures cause selective time-dependent changes to adult-generated hippocampal dentate granule cells. J Neurosci 2007;27:7541–7552. [PubMed: 17626215]

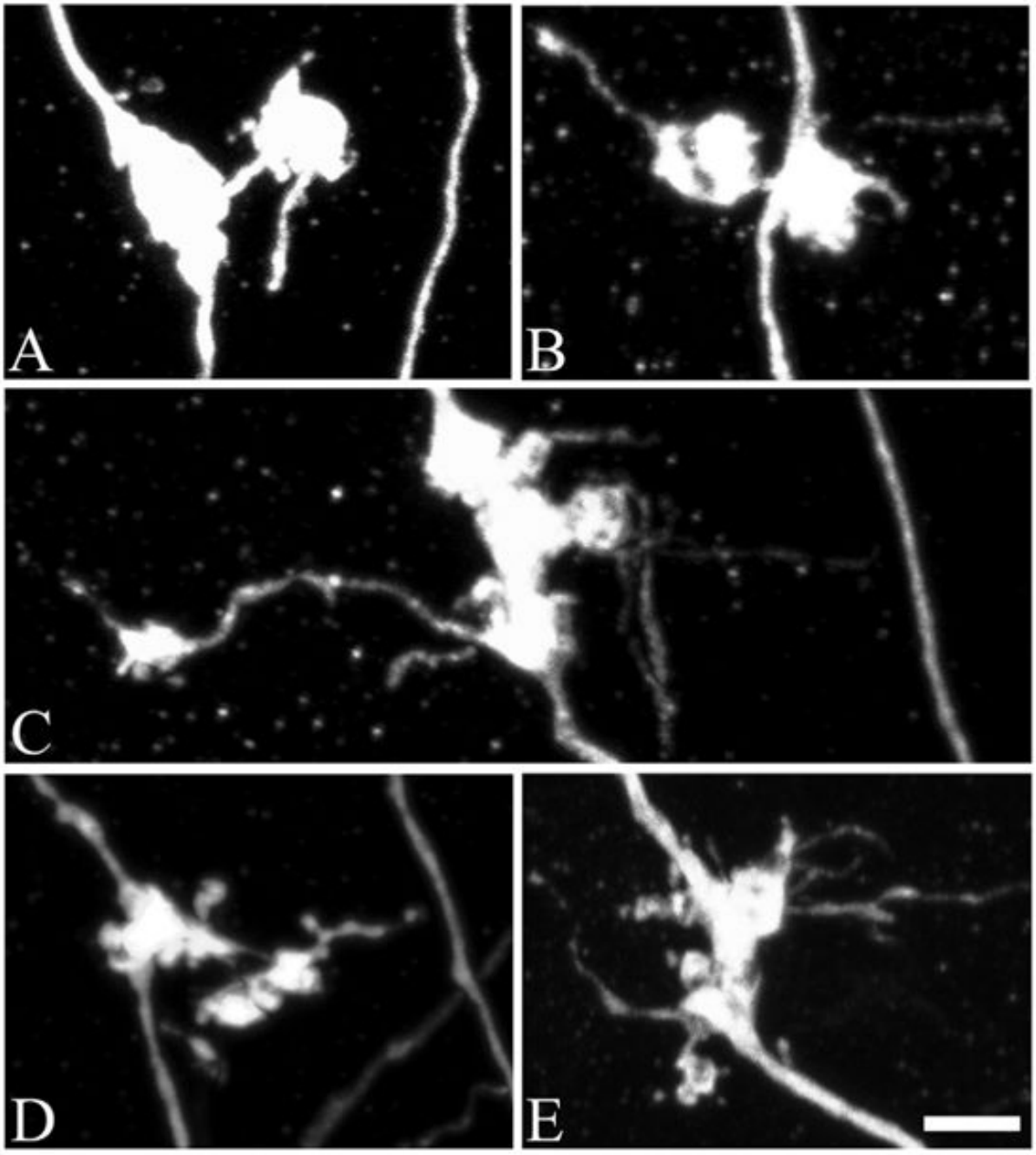

FIGURE 1.

Confocal reconstructions of granule cell giant mossy fiber bouton complexes, which are comprised of a core giant bouton connected to one or more satellite boutons. A, An example of a giant mossy fiber bouton complex from a control animal. In controls, these complexes were rarely observed. B, Two days after status epilepticus, the incidence of giant mossy fiber boutons with satellites was increased 153% over control values ($P = 0.049$). C–E, One month after status, the percentage of giant mossy fiber boutons connected to satellite boutons was increased 461% over control values ($P = 0.009$). Scale bar = 3 μm. [Color figure can be viewed in the online issue, which is available at www.interscience.wiley.com.]

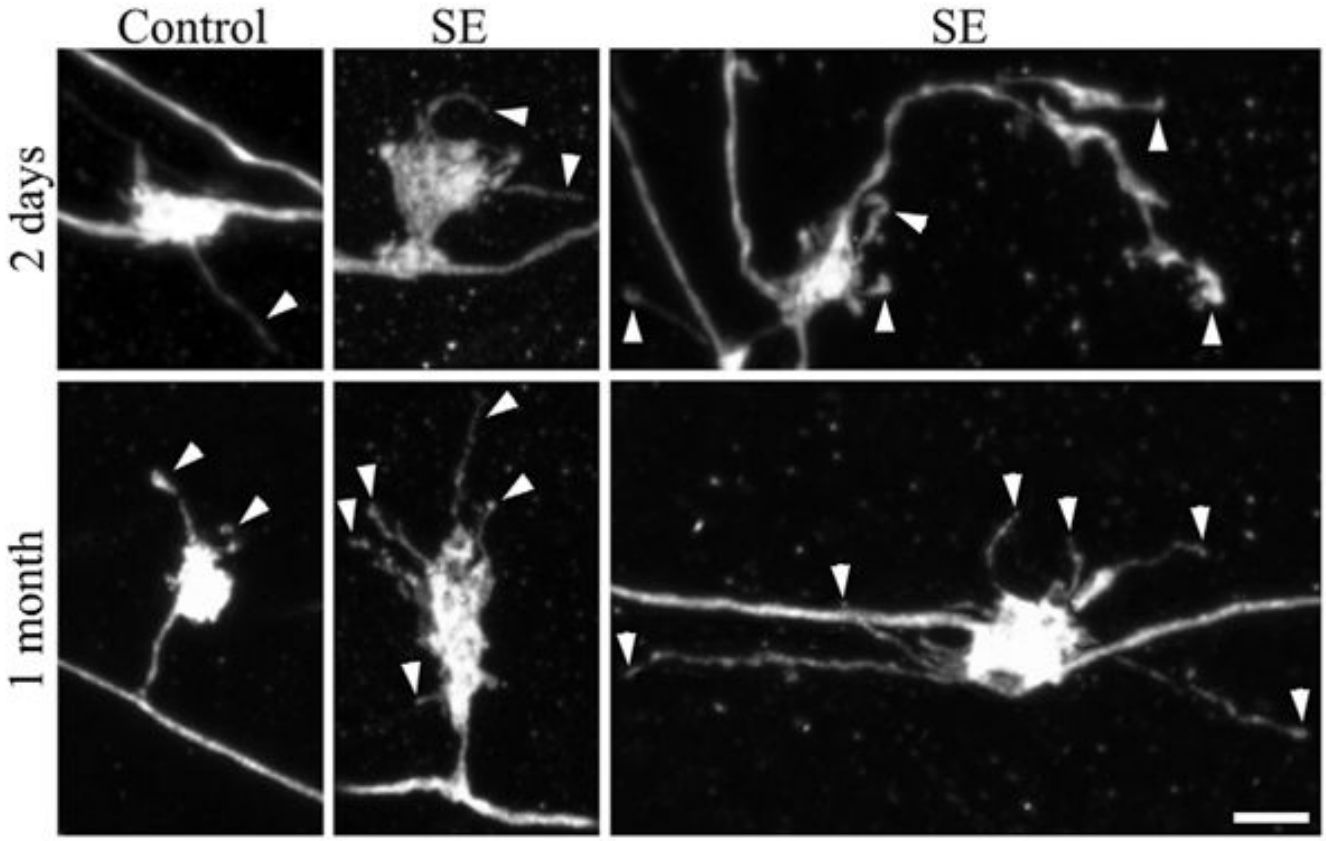

FIGURE 2.

Confocal reconstructions of granule cell giant mossy fiber boutons. Giant boutons are from control animals and animals that underwent status epilepticus (SE) either 2 days or 1 month earlier. The 1 month animals shown exhibited minimal loss of hippocampal principal neurons after status epilepticus (Cumulative damage score = 2). Two days after status epilepticus, the number of filopodia per giant mossy fiber bouton was significantly increased (arrowheads). One month after status epilepticus, giant mossy fiber bouton area, the number of filopodia per giant mossy fiber bouton (arrowheads), and filopodia length were significantly increased relative to age-matched saline controls. Scale bar = 3 μm. [Color figure can be viewed in the online issue, which is available at www.interscience.wiley.com.]

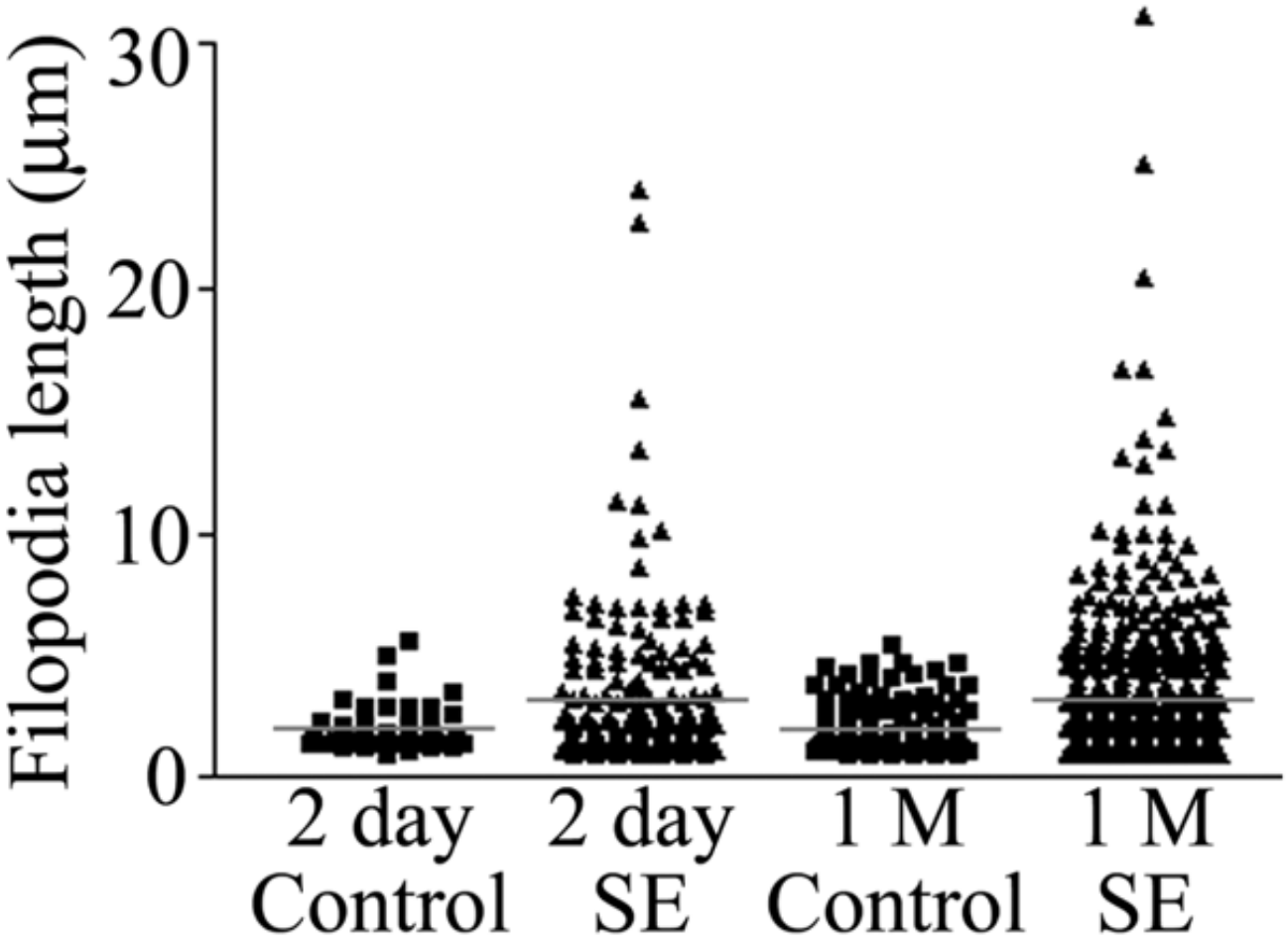

FIGURE 3.

Scatter plot depicting individual filopodia lengths from pilocarpine-treated animals killed 1 day and 1 month (1 M) after status epilepticus (SE). Corresponding control groups are shown as well. Red bars depict the means for each group. Means were generated from the average filopodia length for each animal rather than the raw data shown here (to avoid statistical analyses of nonindependent variables). Although average filopodia length was statistically increased only at the 1 month time point ($P = 0.002$), note the impressive increase in the number of very long filopodia following status at both time points. [Color figure can be viewed in the online issue, which is available at www.interscience.wiley.com.]

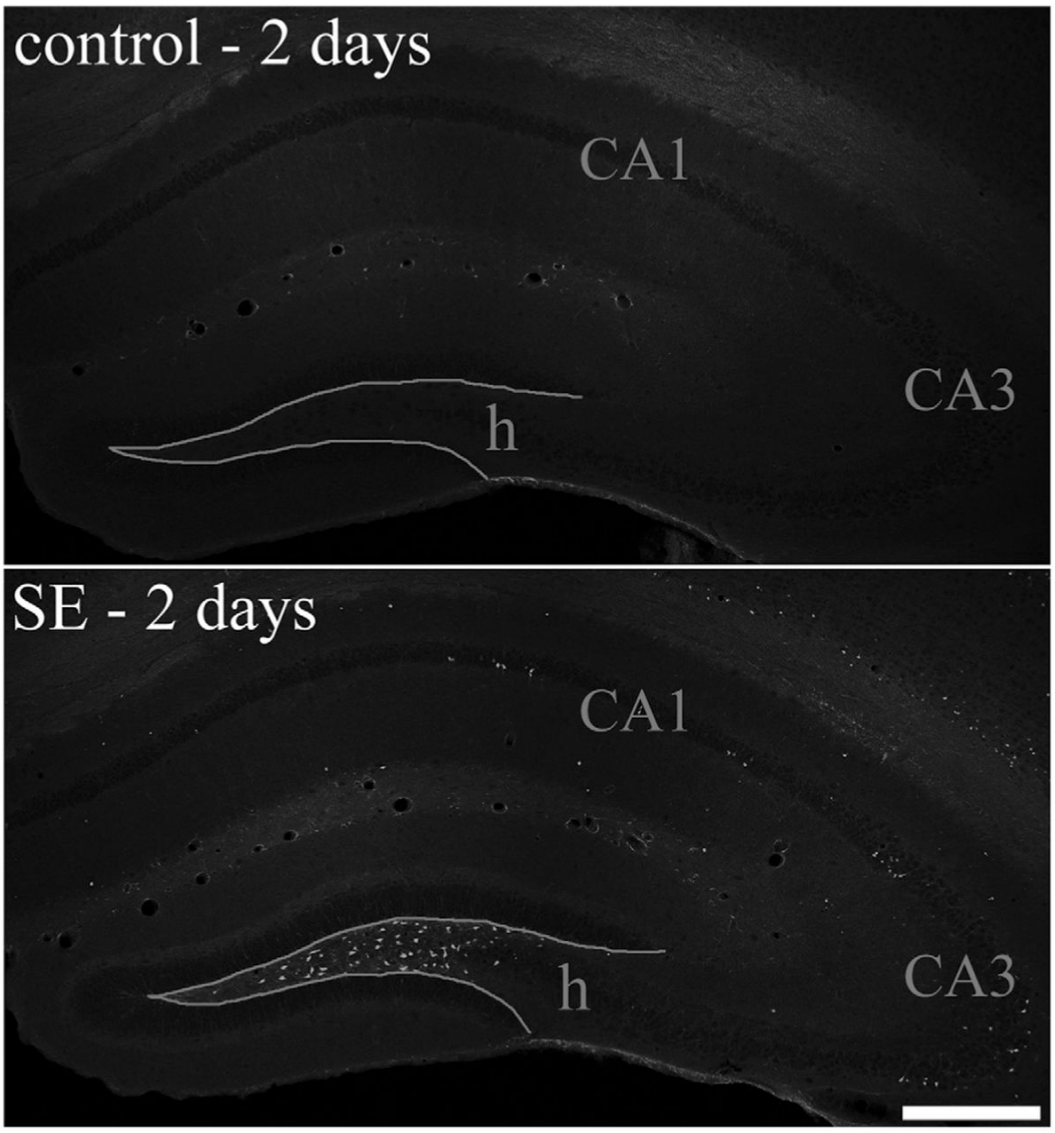

FIGURE 4.

Fluoro-Jade B staining of hippocampal sections from a control animal and pilocarpine-treated animal sacrificed 2 days after status epilepticus (SE). Fluoro-Jade B staining was absent from control animals (top), whereas in pilocarpine-treated animals large numbers of labeled cells were present in the dentate hilus (h) and scattered cells were labeled throughout the CA1 and CA3 pyramidal cell layers. Scale bar = 300 μm. [Color figure can be viewed in the online issue, which is available at www.interscience.wiley.com.]

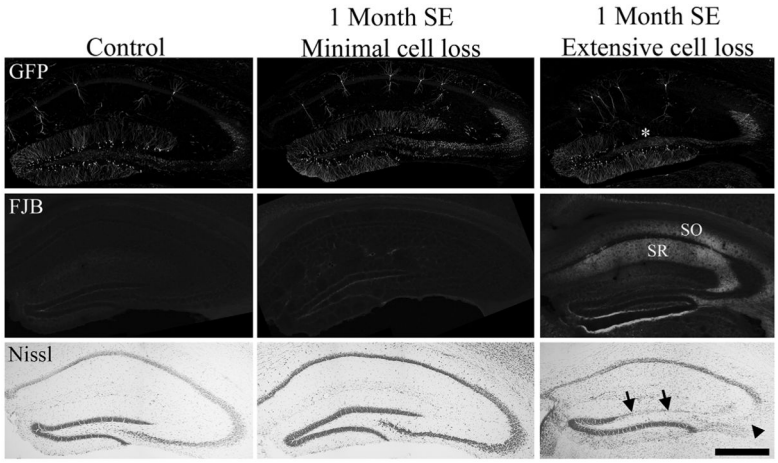

FIGURE 5.

Green fluorescent protein (GFP), Fluoro-Jade B (FJB), and cresyl violet (Nissl) staining in a 1 month saline control mouse (left column) and mice 1 month after pilocarpine-induced status epilepticus (SE). The middle column shows sections from an animal with no detectable loss of dentate granule cells, CA3 pyramidal cells or CA1 pyramidal cells (cell loss score = 2 due to hilar damage). The right column shows sections from an animal (cell loss score = 8) with obvious loss of dentate granule cells (arrows) and CA3 pyramidal cells (arrowhead). Loss of GFP labeling, reflecting granule cell death, is also evident in the DG of this animal (asterisk). Fluoro-Jade B staining reveals degenerating fibers in stratum radiatum (SR) and stratum oriens (SO) of CA1 in this animal. Staining on the lower edge of the dentate and upper edge of the adjacent thalamus is artifactual ("edge artifact"). Scale bar = 500 μm. [Color figure can be viewed in the online issue, which is available at www.interscience.wiley.com.]

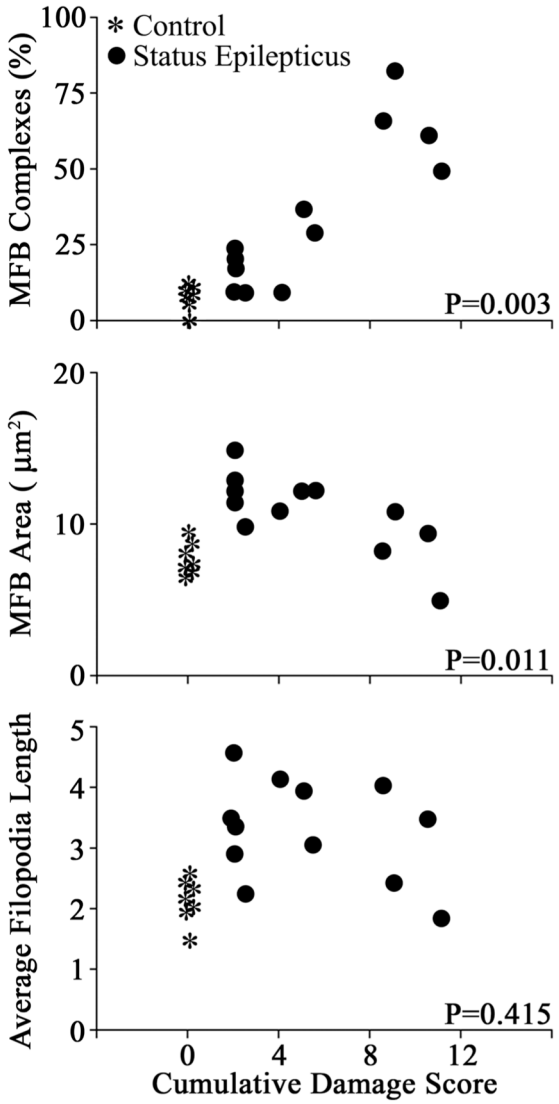

FIGURE 6.

Scatter plots showing significant correlations between loss of hippocampal neurons and changes in granule cell morphology. Cumulative damage score equals the combined semi-quantitative cell loss scores for the DG, hilus, CA1, and CA3 pyramidal cell layers (no loss = 0; >90% loss in all four regions = 12). Among pilocarpine treated animals (black dots), cumulative damage scores were significantly correlated with the percentage of giant mossy fiber boutons with satellites (MFB complexes) and MFB area. Although control animals are depicted in the scatter plots (asterisks), they were not included in the statistical analyses used to generate significant correlations. In the case of MFB complexes, inclusion of control animals produced even stronger correlations, as is evident in the plot. In the case of MFB area, intriguingly, inclusion of control animals revealed a bimodal effect of cell loss. By way of contrast, although giant mossy fiber bouton filopodia length was significantly increased 1 month after status relative to controls, this variable exhibited no correlation with cell loss among pilocarpine-treated animals. Each symbol represents an individual animal.

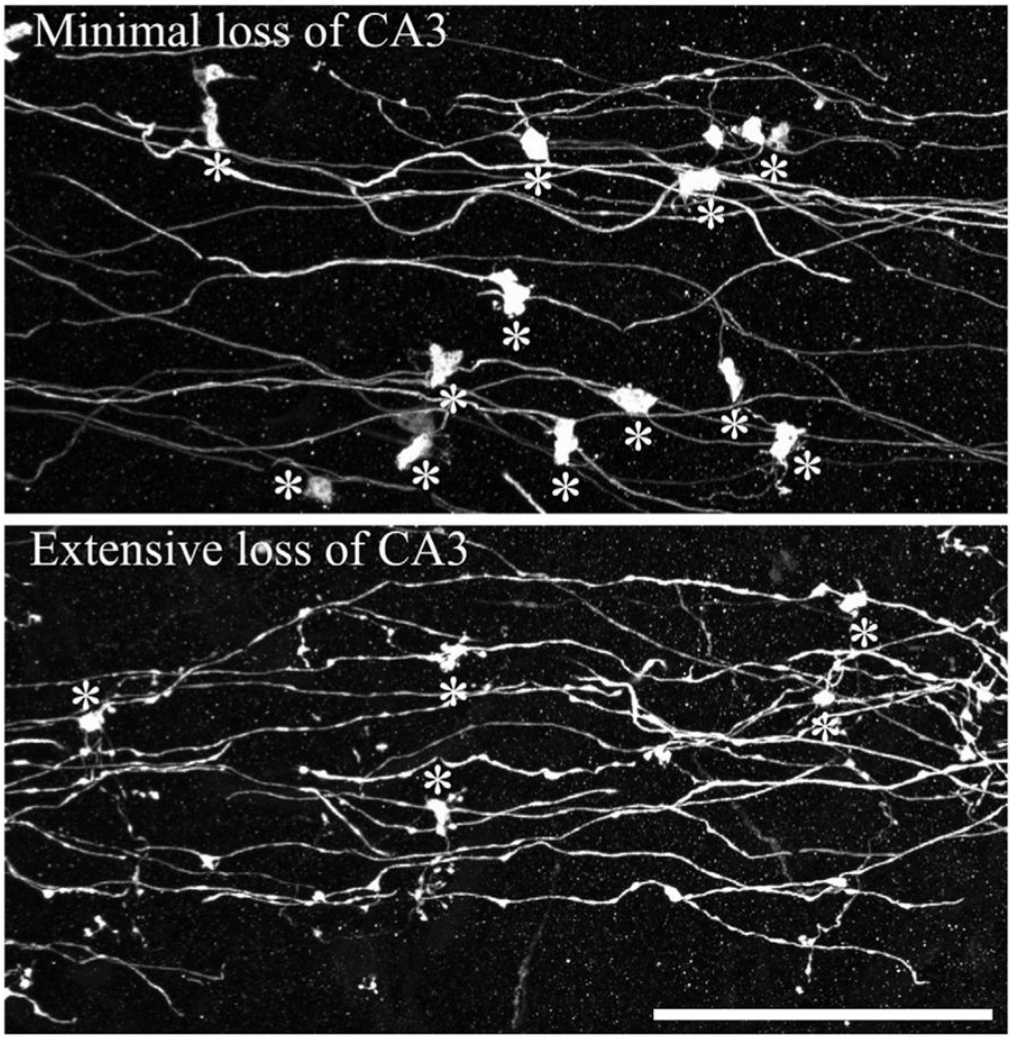

FIGURE 7.
Confocal reconstructions of dentate granule cell mossy fiber axons from animals collected 1 month after status epilepticus. Animals with minimal (top) and extensive (bottom) cell loss are shown. Asterisks denote giant mossy fiber boutons. Note the smaller size of giant boutons from the animal exhibiting extensive cell loss, and the beaded appearance of the attached axons. Scale bar = 40 μm. [Color figure can be viewed in the online issue, which is available at www.interscience.wiley.com.]

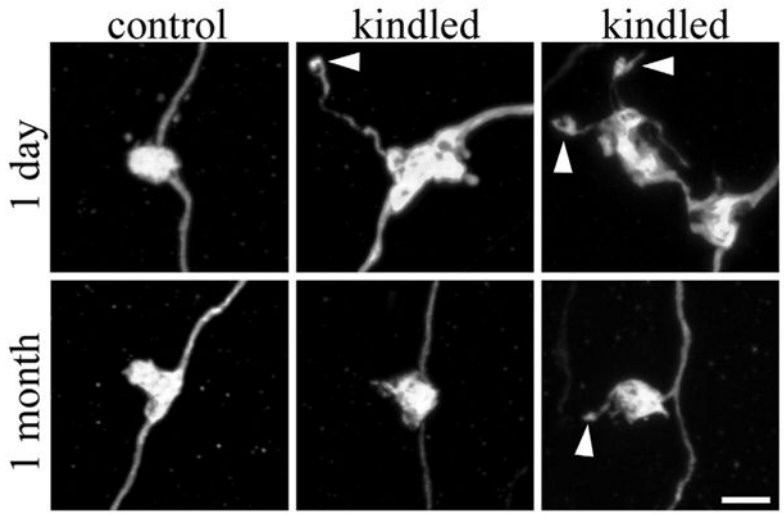

FIGURE 8.

Confocal reconstructions of granule cell giant mossy fiber boutons. Giant boutons are from control animals and amygdala-kindled animals either 1 day or 1 month after the last evoked seizure. One day after the last evoked seizure, giant mossy fiber bouton area, the number of filopodia per giant mossy fiber bouton (arrowheads), and the length of these filopodia were significantly increased relative to control animals. These changes, however, were transient. One month after the last evoked seizure, giant mossy fiber boutons from kindled animals were indistinguishable from controls. Scale bar = 3 μm. [Color figure can be viewed in the online issue, which is available at www.interscience.wiley.com.]

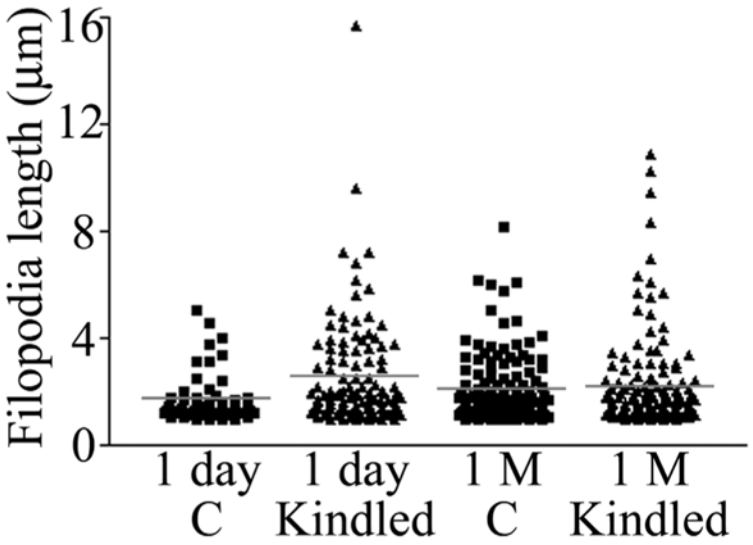

FIGURE 9.

Scatter plot depicting individual filopodia lengths from control animals (C) and kindled animals sacrificed 1 day and 1 month (1 M) after the last evoked seizure. Mean filopodia length (red bar) was significantly increased 1 day, but not 1 month, after the last evoked seizure. Notably, although mean filopodia length was increased, the longest filopodia were still only half the length of the longest filopodia observed in animals exposed to status epilepticus (compared with Fig. 3). [Color figure can be viewed in the online issue, which is available at www.interscience.wiley.com.]

TABLE 1

Pilocarpine-Status Epilepticus

	2 Days control (*N* = 4)	2 Days post-status (*N* = 6)	1 Month control (*N* = 7)	1 Month post-status (*N* = 12)
MFB density (MFB per 100 μm)	0.94 ± 0.12	0.91 ± 0.12	0.76 ± 0.06	0.61 ± 0.09
MFB with satellites (%)	**4.82 ± 2.39 (3 of 97)**[a]	**12.19 ± 2.05**[*] **(12 of 102)**[a]	**6.22 ± 1.72 (16 of 239)**[a]	**34.92 ± 7.27**[**] **(63 of 254)**[a]
MFB area (μm^2)	8.21 ± 0.31	8.87 ± 0.75	**7.94 ± 0.39**	**10.85 ± 0.73**[**]
Filopodia No. per MFB	**1.09 ± 0.27**	**2.34 ± 0.40**[*]	**1.54 ± 0.26**	**3.41 ± 0.42**[**]
Average filopodia length	2.35 ± 0.17	3.16 ± 0.40	**2.08 ± 0.12**	**3.30 ± 0.24**[**]

Morphological measures from age-matched control and pilocarpine-treated mice examined 2 days and 1 month after status epilepticus. Values are means ± standard error.

Significant values are in bold.

MFB, giant mossy fiber bouton.

[*] $P < 0.05$.

[**] $P < 0.01$ (*t*-test).

[a] Number of giant boutons with satellites relative to the total number of boutons examined. Note that percentages calculated from these numbers will differ slightly from percentages calculated from animal means.

TABLE 2

Amygdala Kindling

	24 h Control (*N* = 7)	24 h Post-kindling (*N* = 7)	1 Month control (*N* = 8)	1 Month post-kindling (*N* = 7)
MFB Density (MFB per 100 μm)	0.65 ± 0.07	0.80 ± 0.06	0.70 ± 0.05	0.71 ± 0.04
MFB with satellites (%)	7.76 ± 2.04 (13 of 154)[a]	10.31 ± 2.42 (21 of 196)[a]	5.63 ± 2.45 (10 of 193)[a]	10.25 ± 2.16 (14 of 193)[a]
MFB area (μm^2)	**7.72 ± 0.71**	**11.46 ± 1.08**[*]	9.33 ± 0.60	9.47 ± 0.77
Filopodia No. per MFB	**1.11 ± 0.19**	**1.79 ± 0.23**[*]	1.61 ± 0.17	1.79 ± 0.18
Average filopodia length	**1.85 ± 0.17**	**2.59 ± 0.19**[*]	2.23 ± 0.18	2.30 ± 0.18

Morphological measures from control mice and age-matched kindled mice examined 24 h and 1 month after the last evoked seizure. Values are means ± standard error. Significant values are in bold.

MFB, giant mossy fiber bouton.

[*] $P < 0.05$ (*t*-test).

[a] number of giant boutons with satellites relative to the total number of boutons examined. Note that percentages calculated from these numbers will differ slightly from percentages calculated from animal means.